Chemical and Electrochemical Insertion of Lithium into Two Allotropic Varieties of $NbPO_5$

Sébastien Patoux† and Christian Masquelier*,†

Laboratoire de Réactivité et de Chimie des Solides, CNRS UMR 6007, Université de Picardie Jules Verne, 33 rue Saint-Leu, 80039 Amiens Cedex, France

Received December 5, 2001. Revised Manuscript Received February 13, 2002

The chemical and electrochemical insertions of lithium into α-$NbPO_5$ ($P4/n$) and β-$NbPO_5$ ($P2_1/c$) are compared. Both materials were evaluated as positive electrodes in lithium-type rechargeable batteries through galvanostatic, GITT, and PITT cycling modes within various voltage windows. They present distinct behaviors with regard to lithium insertion. β-Li_x-$NbPO_5$ rapidly and reversibly uptakes lithium leading to a sustained capacity of 90−120 mA·h/g (i.e., operating to the Nb^{5+}/Nb^{4+} couple) for more than 100 cycles at ∼2 V vs Li^+/Li. This reversibility was confirmed by in situ X-ray diffraction in the range $0 \le x \le 0.7$ that additionally revealed a series of single- and two-phase insertion mechanisms. On the other hand, α-Li_xNbPO_5 displays an insertion plateau at ∼1.7 V vs Li^+/Li indicative of a two-phase process that was found to be poorly reversible. Both materials, when discharged at voltages lower than 1 V, present irreversible reactions with complete amorphization.

I. Introduction

Following Padhi et al. studies,[1−5] polyanionic frameworks associated with different transition metal elements have been considered as electrode components for lithium or lithium-ion batteries. This class of materials benefits from the polyanion inductive effect. This effect increases the redox potential of the transition metal element as compared to simple oxides of transition elements. Such inductive effect was further exemplified by Gaubicher's studies on VXO_5-type systems (X = P, As, S), which resulted in the identification of new lithiated Li_xVXO_5 phases.[6−9]

In this context, we decided to explore the electrochemical and structural properties of two allotropic niobium phosphates having the $NbPO_5$ composition (α-$NbPO_5$ and β-$NbPO_5$), previously isolated by Hahn.[10] A phase transition was shown to occur around 1500−1600 K from α-$NbPO_5$ (tetragonal $P4/n$)[11,12] to β-$NbPO_5$ (monoclinic, $P2_1/c$).[13,14] Although still controversial, the existence of a third allotropic form, ϵ-$NbPO_5$ (orthorhombic)[15,16] was reported from a single-crystal investigation in the K−Nb−P−O system.[17] The reported structure is very close to that of the β-form with a similar connection between NbO_6 octahedra and PO_4 tetrahedra.

Among the complex polyanionic framework groups built of MO_6 octahedra (M = Nb, W, Mo, V...) and XO_4 tetrahedra (X = P, S, Mo...), the crystal structure of α-$NbPO_5$ is built on one of the simplest arrangements. It is described in the space group $P4/n$ ($Z = 2$) with $a = 6.388(1)$ Å and $c = 4.118(1)$ Å. The structure consists of PO_4 tetrahedra sharing their corners with NbO_6 octahedra, which themselves share four vertexes with tetrahedra and two with other similar octahedra along [001]. Thus, the α-$NbPO_5$ structure can be described as ..O−Nb−O−Nb−O−... type chains, which are cross-linked by PO_4 forming a three-dimensional network (Figure 1a). The formulation $NbO(PO_4)$ accounts for this peculiar connectivity. The NbO_6 octahedra are distorted with four medium Nb−O−(P) bond lengths (1.97 Å) in the (**a**,**b**) plane, one longer (2.32 Å) and one shorter (1.78 Å), alternately along the **c**-axis (−O−Nb−O− sequences). The latter two distances are unpredicted by Brown's type calculations,[18] contrary to the four other Nb−O−(P) bonds. Similar features are encountered for

* To whom correspondence should be addressed.
† E-mail: sebastien.patoux@sc.u-picardie.fr; christian.masquelier@sc.u-picardie.fr.

(1) Padhi, A. K. Ph.D. Thesis, The University of Texas at Austin, 1997.
(2) Padhi, A. K.; Nanjundaswamy, K. S.; Masquelier, C.; Okada, S.; Goodenough, J. B. *J. Electrochem. Soc.* **1997**, *144* 1609−1613.
(3) Padhi, A. K.; Nanjundaswamy, K. S.; Masquelier, C.; Goodenough, J. B. *J. Electrochem. Soc.* **1997**, *144*, 2581−2586.
(4) Padhi, A. K.; Nanjundaswamy, K. S.; Goodenough, J. B. *J. Electrochem. Soc.* **1997**, *144*, 1188.
(5) Nanjundaswamy, K. S.; Padhi, A. K. Goodenough, J. B.; Okada, S.; Ohtsuka, H.; Arai, H.; Yamaki, J. *Solid State Ionics* **1996**, *92*, 1−10.
(6) Gaubicher, J.; Chabre, Y.; Argenault, J.; Lautié, A.; Quarton, M. *J. Alloys Compd.* **1997**, *262−263*, 34−38.
(7) Gaubicher, J.; Le Mercier, T.; Chabre, Y.; Angenault, J.; Quarton, M. *J. Electrochem. Soc.* **1999**, *146*, 4375−4379.
(8) Ker, T. A.; Gaubicher, J.; Nazar, L. *Electrochem. Solid State Lett.* **2000**, *3*, 460−462.
(9) Gaubicher, J.; Orsini, F.; Le Mercier, T.; Llorente, S.; Villesuzanne, A.; Angenault, J.; Quarton, M. *J. Solid State Chem.* **2000**, *150*, 250−257.
(10) Hahn, R. B. *J. Am. Chem. Soc.* **1951**, *73*, 5091.
(11) Longo, J. M.; Kierkegaard, P. *Acta Chem. Scand.* **1966**, *20*, 72−78.
(12) Amos, T. G.; Yokochi, A.; Sleight, A. W. *J. Solid State Chem.* **1998**, *14*, 303−307.
(13) Leclaire, A.; Chahboun, H.; Groult, D.; Raveau, B. *Z. Kristallogr.* **1986**, *177*, 277−286.
(14) Chahboun, H.; Groult, D.; Hervieu, M.; Raveau, B. *J. Solid State Chem.* **1986**, *65*, 331−342.
(15) Chahboun, H.; Groult, D.; Raveau, B. *C. R. Acad. Sci. Paris* **1987**, *304*, 807−810.
(16) Zah-Letho, J. J.; Verbaere, A.; Jouanneaux, A.; Taulelle, F.; Piffard, Y.; Tournoux, M. *J. Solid State Chem.* **1995**, *116*, 335−342.
(17) Serra, D. L.; Hwu, S.-J. *Acta Crystallogr.* **1992**, *C48*, 733−735.
(18) Brown, I. D.; Kang Kun Wu. *Acta Crystallogr.* **1976**, *B32*, 1957.

10.1021/cm010398d CCC: $22.00
Published on Web 04/04/2002

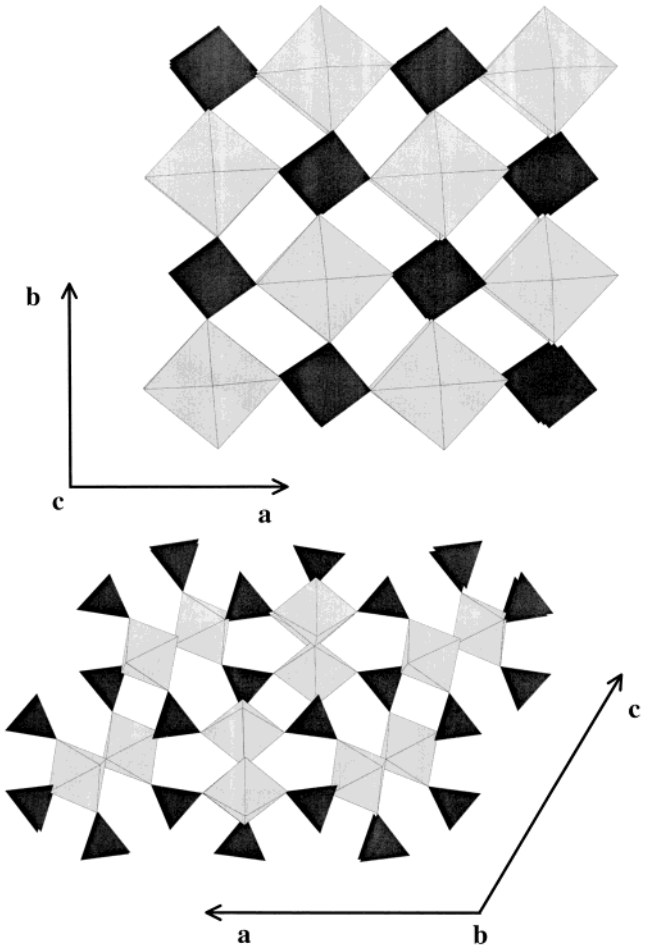

Figure 1. (a) Structure of α-$NbPO_5$ viewed along [001]. (b) Structure of β-$NbPO_5$ viewed along [010].

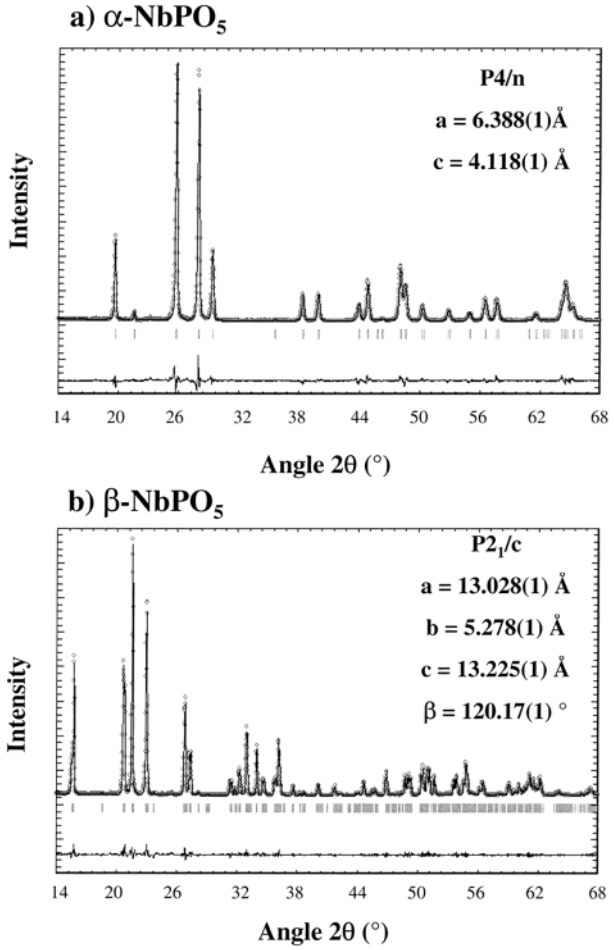

Figure 2. X-ray diffraction profiles of the experimental (circles) and calculated (full lines) patterns following the Rietveld method for (a) α-$NbPO_5$ and (b) β-$NbPO_5$. The vertical lines indicate the possible Bragg positions.

$VOPO_4$ and $MoOPO_4$, which are isostructural with α-$NbPO_5$.

On the other hand, two kinds of more regular NbO_6 octahedra are encountered in β-$NbPO_5$ that crystallizes in the monoclinic space group $P2_1/c$ ($Z = 8$) with $a =$ 13.028(1) Å, $b = 5.278(1)$ Å, $c = 13.225(1)$ Å, and $\beta =$ 120.17(1)°. This second high-temperature form is characterized as the member $m = 2$ of the *"MonoPhosphate Tungsten Bronze with pentagonal tunnels"* ($MPTB_p$) family of general formula $A_x(NbO_3)_{2m}(PO_2)_4$ (A = Li, Na, Ag).[19] The structure is described as ReO_3-type chains of NbO_6 octahedra, separated by slabs of PO_4 tetrahedra delimiting pentagonal tunnels (Figure 1b). In this structure, double strings of NbO_6 octahedra parallel to the **b**-axis are isolated, and linked to others by tetrahedra only.

The purpose of our study was to establish relationships between the structures of α- and β-$NbPO_5$ and their electrochemical properties toward insertion of lithium as these two materials present empty interstitial spaces within their frameworks. As developed in this paper, our investigations were conducted through various electrochemical cycling modes (galvanostatic or potentiostatic) and in situ X-ray diffraction that allowed to follow the phase transformations as x increases in Li_xNbPO_5.

(19) Patoux, S.; Masquelier, C., in preparation.

II. Experimental Section

The synthesis of polycrystalline α-$NbPO_5$ was made according to a "gel route" already published for MVO_5 (M = Nb, Ta).[20] A gel was obtained by dispersing a solution of $NbCl_5$ in ethanol ($NbCl_5$ was weighed under an argon atmosphere to avoid the rapid formation of HCl due to the high air sensitivity of $NbCl_5$ toward water), to which was added an aqueous solution of $NH_4H_2PO_4$ using stoichiometric proportions. A white/yellow opaque gel instantaneously formed as soon as the reagents were mixed. The gel was stirred and kept at 323−333 K until complete drying for about 1 day. After grinding and heating at 873 K (24 h) and 1173−1273 K (24 h), a pure and well-crystallized α-$NbPO_5$ phase was obtained, in agreement with a TGA-DTA preliminary experiment (Setaram 92b device). By using this "gel" method, an excess of phosphorus was not needed, as compared to what was reported before.[12] Nevertheless, this "wet" homogenization method did not allow the synthesis of the pure β-phase polymorph. Traces of a secondary phase such as PNb_9O_{25} are always present, mostly due to the high temperature required by the preparation of a pure β-powder.

The second allotropic form, β-$NbPO_5$, was obtained by a classical solid state reaction mostly similar to that previously reported.[21] Nb_2O_5 (Aldrich, 99.99%) plus a large excess (three times the stoichiometric amount required) of $NH_4H_2PO_4$ (NORMAPUR, min 98%) was needed due to the volatilisation

(20) Amarilla, J.-M.; Casal, B.; Galvan, J.-C.; Ruiz-Hitzky, E. *Chem. Mater.* **1992**, *4*, 62−67.

(21) Benabbas, A.; Borel, M. M.; Grandin, A.; Leclaire, A.; Raveau, B. *J. Solid State Chem.* **1991**, *95*, 245−252.

of P_2O_5 at high temperatures. The mixture was carefully mixed and slowly heated (1 K/min) first up to 573 K for 3 h for H_2O and NH_3 to evaporate. After an intermediate treatment at 873 K and subsequent grinding, a pure and well-crystallized sample was obtained by a thermal treatment of 12 h at 1623 K followed by a rapid quench in air.

The lattice parameters and atomic positions of the two single-phase powders were determined by the Rietveld method with the WinPLOTR/Fullprof suite[22] from X-ray diffraction data recorded overnight on a Philips PW1710 diffractometer (Cu Kα radiation) (Figure 2a,b). From scanning electron microscopy (FEG XL30) observations, the two powders are pretty similar, shape wise, and present heterodispersed particles.

The two orthophosphates were tested as positive electrode materials in Swagelok-type cells assembled in an argon-filled drybox with Li metal as the negative electrode and a Whatman GF/D borosilicate glass fiber sheet saturated with a 1 M $LiPF_6$ in ethylene carbonate (EC): dimethyl carbonate (DMC) (1:1 in weight) as the electrolyte. The composite positive electrodes were prepared by either mixing in an agate mortar or in a ball-miller the active material (AM) with 16.67 wt % of carbon Super P (SP, MMM Carbon, Belgium) to improve electronic conductivity. Lithium insertion/extraction was monitored with a "Mac-Pile" automatic cycling/data recording system (Biologic SA, Claix, France) operating in galvanostatic, GITT (galvanostatic intermittent titration technique) or PITT (potentiostatic intermittent titration technique) modes.

Electrochemically-driven structural changes were followed by means of an in situ electrochemical cell similar to that previously described,[23] and having a plastic film of the positive electrode material deposited behind a beryllium window, which acted as the positive current collector. The preparation of the plastic films was done as previously reported for the plastic PLiON (Bellcore) technology film.[24] It contained 55 parts of a AM powder, 8 parts of carbon SP, and 22 parts of dibutylphthalate (DBP) dispersed in 15 parts of (poly) vinylidene-hexafluoropropylene (PVdF−HFP) (Kynar FLEX, Elf Atochem NA). In some cases, the AM and carbon SP were previously ball-milled to favor electrical conductivity. Once assembled, the cell was then mounted on a Scintag diffractometer operating in Bragg−Brentano geometry with a Cu Kα radiation, and connected to the Mac-Pile system operating in a GITT mode, with discharge/charge periods of 1 h at C/10 rate separated by a 1.5 h relaxation period during which an X-ray diffraction pattern was recorded. For better resolution an additional in situ experiment was performed using a D8 (BRUKER) diffractometer using Co Kα radiation in $\theta-\theta$ reflection mode. In that case, the GITT protocol consisted of sequences of 30 min of discharge or charge at C/20 separated by relaxation periods of 2 h.

Chemical lithiations of the two samples were performed using an excess of *n*-BuLi (1.6 M) in a solution of hexanes. The reactions were maintained under constant stirring at ambient temperature in a flask kept in an argon-filled glovebox for a period of 5 days and subsequently washed many times with hexanes before drying under vacuum. Due to the moisture sensitivity of these lithiated phases, the XRD data were taken using an airtight cell similar to that used for in situ studies. Chemical analysis was then performed at the Service Central d'Analyse du CNRS (Vernaison, France) to deduce the extent of the lithiation. The following formulas "α′-$Li_{3.4}NbPO_5$" and "β'-$Li_{1.2}NbPO_5$" were obtained.

III. Results and Discussion

The electrochemical reaction of lithium with α-$NbPO_5$ and β-$NbPO_5$, between 3.20 and 0.02 V vs Li^+/Li, is presented in parts a and b, respectively, of Figure 3.

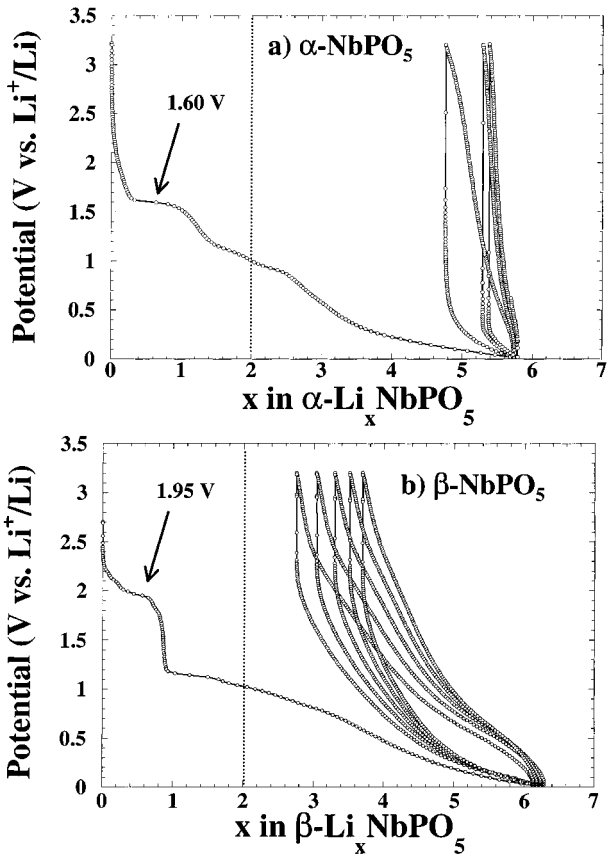

Figure 3. Potential−composition curves for (a) α-$NbPO_5$ and (b) β-$NbPO_5$ obtained from galvanostatic cycling between 3.20 and 0.02 V vs Li^+/Li at a nominal C/10 regime.

Vertical dotted lines are drawn at $x = 2$ to indicate the theoretical Li_2NbPO_5 intercalated compositions for which Nb would be at the oxidation state +3. The voltage−composition profiles reveal that both materials exchange approximately six electrons on the first discharge down to 0.02 V. This value is higher than the theoretical one of five electrons to fully reduce Nb^{5+} to Nb metal. Such a phenomenon has been encountered for several oxide compounds,[25,26] which are decomposed at low potential and from which the extra capacity may arise from carbon reduction and/or formation of passivation layers[27] from electrolyte decomposition below 1 V vs Li^+/Li. As clearly seen in Figure 3, a large irreversibility (>40%) on subsequent charges/discharges is encountered when the materials are initially discharged down to 0.02 V. Ex situ X-ray diffraction on samples discharged below 1 V indicates a complete destruction of the $NbPO_5$ frameworks and no further recrystallization on the following charge up to 3.2 V.

The two forms of $NbPO_5$ differ in the redox processes that occur in the 2.5−1.4 V vs Li^+/Li voltage window. As shown by the ($-\partial x/\partial U = f(U)$) derivative curves on Figure 4, these redox processes are located at 1.65 V for α-$NbPO_5$ and at 2.15, ∼2.00 and 1.85 V for β-$NbPO_5$. It is important to note that it was necessary to optimize the AM/carbon SP composite electrode to observe these

(22) Roisnel, T.; Rodriguez-Carvajal, J. *WinPLOTR; May, 2000.* downloadable at: http://www-llb.cea.fr/fullweb/powder.htm.
(23) Amatucci, G. G.; Tarascon, J.-M.; Klein, L. C. *J. Electrochem. Soc.* **1996**, *143*, 3.
(24) Tarascon, J.-M.; Gozdz, A. S.; Schmutz, C.; Warren, P. C. *Solid State Ionics* **1996**, *86*, 49.
(25) Baudrin, E.; Laruelle, S.; Denis, S.; Touboul, M.; Tarascon, J. M. *Solid State Ionics* **1999**, *123*, 139−153.
(26) Patoux, S.; Vannier, R.-N.; Mairesse, G.; Nowogrocki, G.; Tarascon, J. M. *Chem. Mater.* **2001**, *13*, 500−507.
(27) Poizot, P.; Laruelle, S.; Grugeon, S.; Dupont, L.; Tarascon, J. M. *Ionics* **2000**, *6*, 321−330.

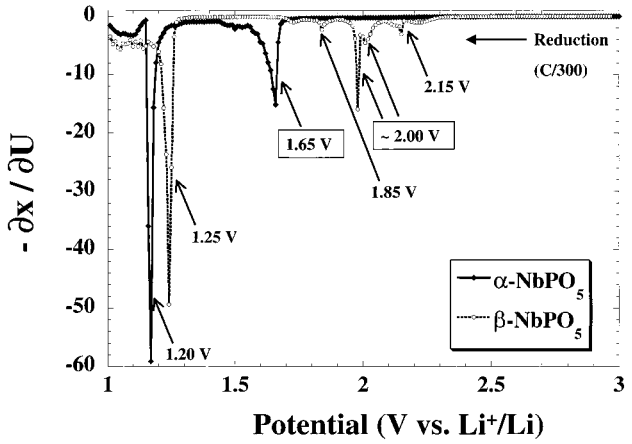

Figure 4. Incremental capacity curve for α-$NbPO_5$ (full line) and β-$NbPO_5$ (dashed line) vs Li^+/Li on the first discharge (~C/300).

redox steps for α-$NbPO_5$. Such optimization was done through a 20 min ball-milling of a mixture α-$NbPO_5$ plus carbon by means of a SPEX 8000 mixer that generates impacts/shocks and favors then electronic contact.

PITT measurements were undertaken down to 1.1 V for both materials. From such experiments, the two-phase domains are easy recognizable by their bell-shaped chronoamperometric responses. Discharge was done through potential increments of 10 mV, with voltage changes occurring when the absolute value of the current reached a minimal value I_{min} that would correspond to a C/300 regime. The obtained data are plotted in Figure 5a for α-$NbPO_5$ and in Figure 5b for β-$NbPO_5$. Two-phase domains were identified at $x \geq 1.5$ for α-Li_xNbPO_5 and $x \geq 1$ for β-Li_xNbPO_5 when the potential was left to decrease down to 1.1 V vs Li^+/Li. In this low voltage region, in situ and ex situ X-ray diffraction showed a progressive, and non-reversible, amorphization of α′-$Li_{1.5}NbPO_5$ and β′-$LiNbPO_5$ along the discharge plateaus.

As already mentioned, the most interesting parts of the voltage/composition profiles are nested in the low x values, i.e., at $x \leq 1.4$ in α-Li_xNbPO_5 and $x \leq 1$ in β-Li_xNbPO_5. Thus, we studied these domains by means of in situ X-ray diffraction experiments, and the results are shown in Figure 6b and Figure 7b for α-Li_xNbPO_5 and β-Li_xNbPO_5, respectively.

The evolution of the X-ray diffraction patterns, plotted in the 24.00−42.00 2θ(°) range, during "reversible" lithium insertion into α-$NbPO_5$ is shown in Figure 6b. The absence of any shift in the peak positions over the composition range $0 \leq x \leq 0.4$, for which PITT experiments indicate a solid solution insertion process, implies that there is basically no change in lattice parameters. The first discharge intercalation plateau between $x \approx 0.4$ and $x \approx 1.2$ is related to a two-phase domain into which the diffraction peaks characteristic of α-$Li_{0.4}NbPO_5$ vanish for the benefit of those of a new lithiated form of approximate composition α′-$Li_{1.4}NbPO_5$, in agreement with PITT data. The crystallographic features of this new phase, whose peak positions are totally different from those of the β form-type, have not been elucidated yet. Further attempts to isolate and characterize this new α′-$Li_{1.4}NbPO_5$ phase by using chemical lithiation with *n*-BuLi partly failed as the obtained final composition was "$Li_{3.4}NbPO_5$". From the PITT experiment of Figure 5a, and from the fact that smooth amorphization occurs on the plateau after $x = 1.4$ (after $x = 1.0$ for β-$NbPO_5$), we propose that this "$Li_{3.4}NbPO_5$" solid is actually a mixture of an amorphous highly lithiated phase and a crystalline form whose diffraction signature is very similar to that of α′-$Li_{1.4}NbPO_5$**.** The discharge down to $x = 1.2$ is partly reversible as only 0.8 Li could be extracted on the following charge. At the end of the charge up to 3.2 V, the X-ray diffraction pattern indicates that the α-$Li_{0.4}NbPO_5$ structure is mostly recovered but with significant enlargements of the diffraction peaks.

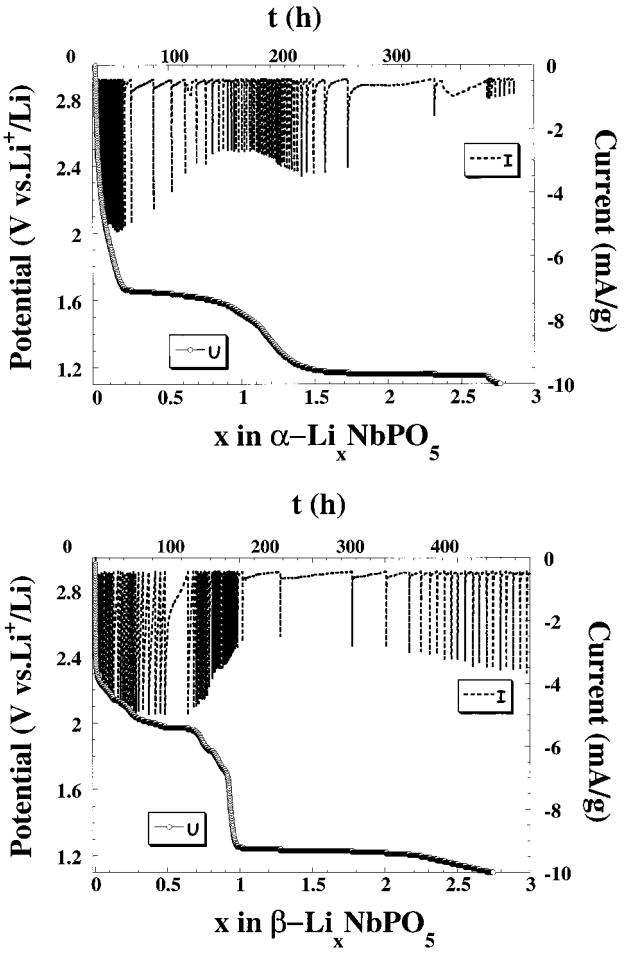

Figure 5. (a) Potentiometric titration curve (PITT) of the first reduction of α-$NbPO_5$ in the 3.20−1.00 V range vs Li^+/Li ($I_{min} = 3.5$ μA). (b) Potentiometric titration curve (PITT) of the first reduction of β-$NbPO_5$ in the 3.20−1.00 V range vs Li^+/Li ($I_{min} = 3.9$ μA).

Similar types of in situ experiments were performed on β-Li_xNbPO_5 in the $0 \leq x < \sim 0.7$ domain, which corresponds to the "2 V process" depicted in Figure 7b. According to the PITT plot of Figure 5b, β-Li_xNbPO_5 shows three intercalation plateaus: two very small ones at $x \sim 0.2$ and $x \sim 0.8$ plus a larger one for $\sim 0.50 \leq x \leq \sim 0.70$. The two small two-phase regions were not identified from the XRD data, and in a first approach lithium insertion into β-$NbPO_5$ proceeds essentially through a solid solution mechanism as shown by the rather continuous shifts in the positions of the diffraction peaks. A careful examination of the XRD patterns recorded in the $\sim 0.50 \leq x \leq \sim 0.70$ domain confirms, according to the PITT data, the presence of a two-phase region process. As shown in the inset plot of Figure 7b

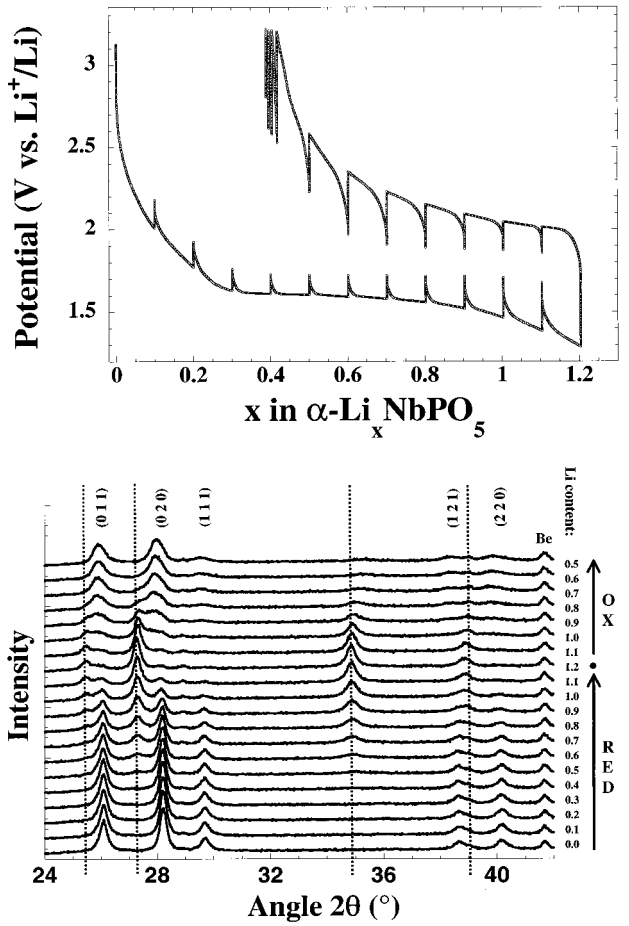

Figure 6. (a) GITT curves of the first cycle of α-$NbPO_5$ obtained in the 3.20−1.30 V range vs Li^+/Li. C/10 regime imposed for 1 h interrupted by relaxation periods of 90 min each. (b) Evolution of the in situ X-ray diffraction patterns of an electrode of α-Li_xNbPO_5 during the first cycle between 3.20 and 1.20 V with an acquisition time of 2 h 30 min (0.12°/min) in the 24.00−42.00 2θ (°) window from a Cu Kα radiation on a Scintag diffractometer. The peak positions of the growing second phase are indicated by vertical dashed lines.

((1 0 2) and ($\bar{3}$ 0 2) peaks), the XRD pattern of the β-Li_xNbPO_5 powder obtained at $x = 0.5$ is much better fitted by the introduction of a second phase, β'-$Li_{0.75}NbPO_5$, coexisting with β-$Li_{0.45}NbPO_5$. The existence of this new β' phase, appearing in the intercalation range $\sim 0.5 \leq x \leq \sim 0.7$, was also suggested by the observation of a break in the lattice parameters variation as a function of x when the XRD pattern is refined as a single monoclinic phase through the whole intercalation range ($0 < x < \sim 0.7$). This in situ experiment performed in the range $0 \leq x \leq 0.7$, showed a nice reversibility of the system when the lower voltage limit is not too small: the diffraction pattern of the material obtained after a full electrochemical cycling (back to a β-$Li_{0.05}NbPO_5$ composition) is essentially the same as that of the pristine material. This is not the case for extended discharge (cutoff voltage ≤ 1.3 V) that generates a partially irreversible amorphization.

To further investigate the mechanism of lithium insertion into β-$NbPO_5$, an additional in situ experiment was performed using a D8-Bruker diffractometer having a θ/θ geometry with a Co Kα radiation. The β-Li_xNbPO_5 ($0 < x < 2.5$) XRD patterns accumulated for 2 h after each change in Δx of 0.05 are shown in Figure 8.

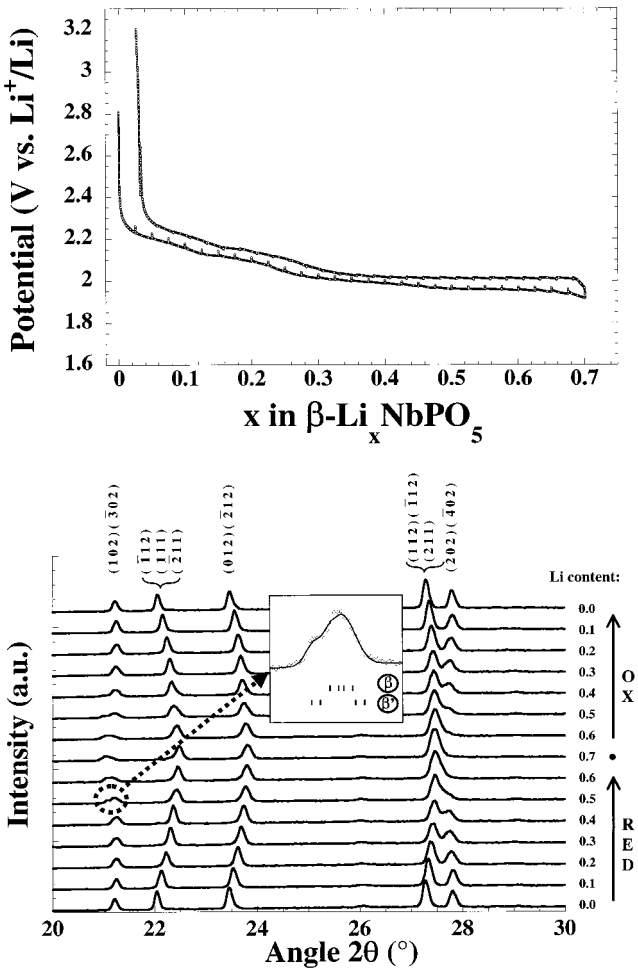

Figure 7. (a) GITT curves of the first cycle of β-$NbPO_5$ obtained in the 3.2−1.0 V range vs Li^+/Li. C/20 regime imposed for 30 min interrupted by relaxation periods of 30 min. (b) Evolution of the in situ X-ray diffraction patterns of an electrode of β-Li_xNbPO_5 during the first cycle between 3.2 and 1.8 V with an acquisition time of 1 h 23 min (0.12°/min) in the 20.00−30.00 2θ (°) window from a Cu Kα radiation on a Scintag diffractometer.

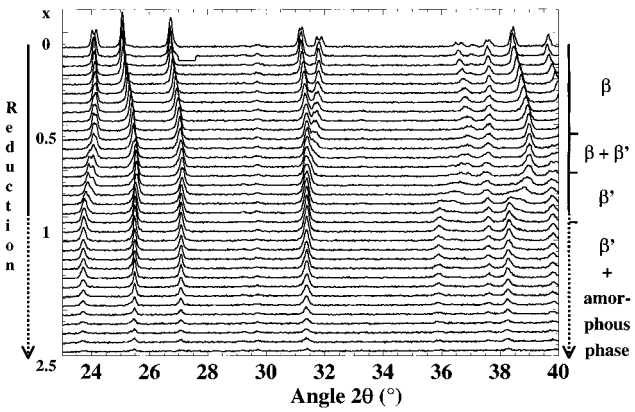

Figure 8. Evolution of the in situ X-ray diffraction patterns of an electrode of β-Li_xNbPO_5 during the first discharge down to 1 V vs Li^+/Li with an acquisition time of 2 h in the 18.00−42.00 2θ (°) range from a Co Kα radiation on a D8-Bruker diffractometer equipped with a PSD counter. Note the misunderstood 1° "counter-break" on the second patterns from the top.

For $x = 0$ (i.e., β-$NbPO_5$), the XRD pattern perfectly matches the monoclinic $P2_1/c$ space group, with unit-cell parameters that leads to a splitting of the (hkl) and

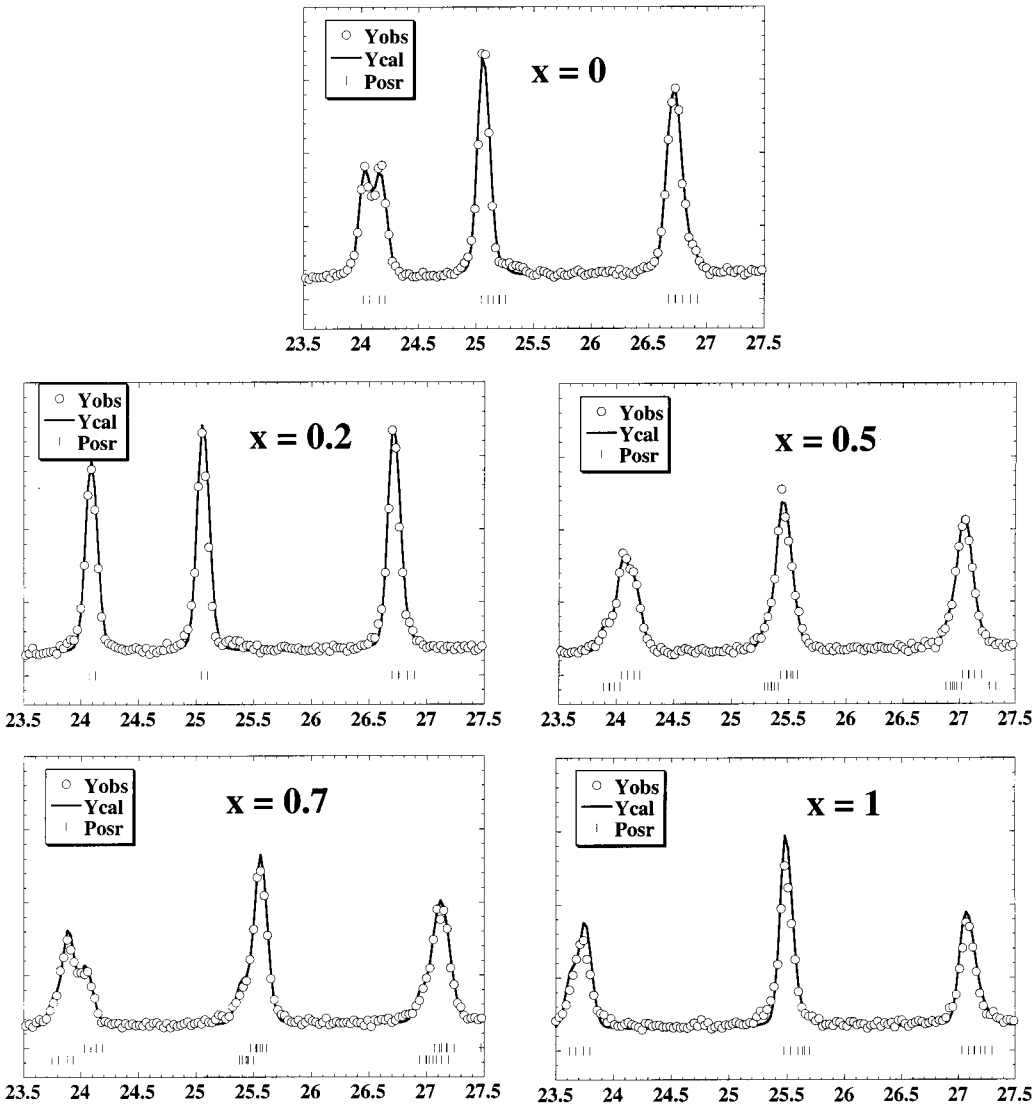

Figure 9. Zoom of the Figure 8 between 23.5 and 27.5 2θ (°) for five distinct values of x in β-Li_xNbPO_5.

$((-h-2n)kl)$ reflections, as seen in Figure 9. As x increases, from 0.05 to 0.50, besides the global shift toward higher angles, some peaks either overlap or split. These peculiar diffraction peaks have the Miller's indices (hkl) and $((-h-2n)kl)$ (e.g., (102) and (−302), (112), and (−312)), which correspond to an exact same value of d_{hkl} when the relation $c = -(a.l.\cos\beta)/n$ (n integer; $l = 2m$) is verified. For specific cell parameters, peak overlapping are reminiscent of a pseudo orthorhombic symmetry ($Pnma$ or $Pn2_1a$ space group) that was already proposed in the literature concerning the pristine material β-$NbPO_5$, from TEM studies. H. Chahboun et al.[14] showed the presence of an orthorhombic ($Pn2_1a$) subcell of the monoclinic ($P2_1/c$) cell whose cell, parameters are linked by the relations: $a_o = a_m \sin\beta$, $b_o = b_m$, and $c_o = c_m/2$.

In the $\sim 0.5 < x < \sim 0.7$ range, β-Li_xNbPO_5 exhibits a two-phase domain (Figure 9) separating two solid solution domains called β and β' for x lower than ~0.45 and x higher than ~0.75, respectively. This two-phase domain is shown in Figure 9 for $x = 0.5$ and 0.7. The β'-type phase, whose lithium content limit was found from chemical lithiation using n-BuLi (1 V vs Li^+/Li), can be indexed in the $P2_1/c$ space group as well. The X-ray diffraction pattern of this new lithiated phase (β' type) may be entirely indexed in the space group $P2_1/c$ with $a = 13.145(3)$ Å, $b = 5.131(1)$ Å, $c = 13.415(3)$ Å, and $\beta = 120.02(1)°$ which, interestingly, corresponds to a unit-cell volume ($V = 783.4$ Å^3) superior to that of the intermediate β' phase compositions but very close to that of the pristine composition β-$NbPO_5$.

As soon as the potential drops to 1.2 V and $x \approx 1.0-1.2$, there is no further shift in the peak positions but the diffracted intensities continuously decrease according to the growth of a second amorphous phase, achieved for $x \approx 2.0-2.5$. This confirms the electrochemical plateau onto which β'-$Li_{1.2}NbPO_5$ coexisted with an amorphous phase as previously discussed from the Figure 5b.

From this comparative study, it appears that α-$NbPO_5$ and β-$NbPO_5$ show two distinct lithium insertion/intercalation processes, especially over the composition range corresponding roughly to the reduction of Nb^{5+} to Nb^{4+}. Although β-Li_xNbPO_5 shows subtle reversible two-phase transitions at intermediate compositions, these phase transitions are much less pronounced than for the α-Li_xNbPO_5 system that is mostly biphasic. A tentative explanation could originate from a compari-

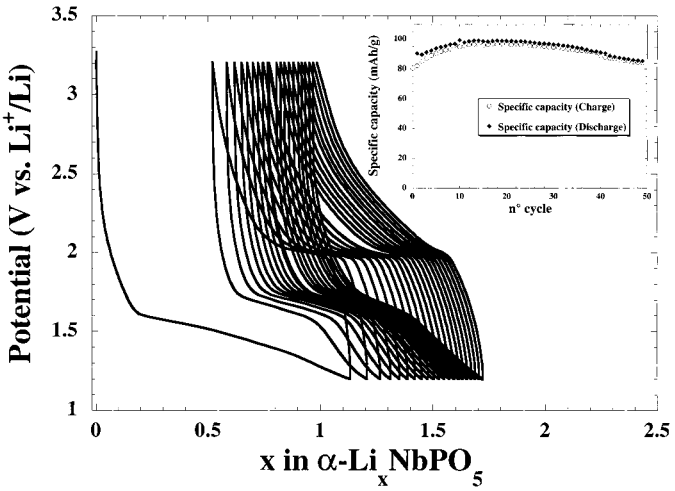

Figure 10. Charge−discharge profile under a galvanostatic mode at current density of C/10 (0.150 mA·h) in the 3.20−1.2 V range vs Li^+/Li for α-Li_xNbPO_5. The *inset plot* represents the evolution of the specific capacity over the first 50 cycles.

son of the gravimetric densities of both structures: 4.04 g cm^{-3} for α-$NbPO_5$ and 3.45 g cm^{-3} for *β*-$NbPO_5$. A wider interstitial space in *β*-$NbPO_5$ (i.e., the smallest density) would tend to favor a smoother reversible lithium insertion. The easier lithium insertion into *β*-$NbPO_5$ as compared to α-$NbPO_5$ is consistent with the smallest polarization displayed by the *β*-$NbPO_5$/Elec./Li cells.

The reversible lithium insertion domains for both forms of $NbPO_5$ correspond to reduction/oxidation onto the Nb^{5+}/Nb^{4+} couple. The position of this couple vs Li^+/Li is situated at ∼1.65 V for α-$NbPO_5$ and at ∼2.0 V for *β*-$NbPO_5$, namely at intermediate values between those already encountered in the NASICON compounds $Li_xNbM(PO_4)_3$, M = Fe or Ti (2.2 V)[3] and in oxides such as PNb_9O_{25} and H−Nb_2O_5 (1.5 V).[28] In light of Gaubicher's work, dealing with the V^{5+}/V^{4+} redox couple in materials of formula Li_xVOPO_4,[7,29] our observation is most likely nested in the peculiar connection between NbO_6 octahedra and PO_4 tetrahedra in the structures of these two $NbPO_5$ compounds, and boils down to J. B. Goodenough's concept of the inductive effect.[30] According to Goodenough, PO_4 groups tend to weaken the M−O bond strengths, and thus increase the operating voltage versus Li^+/Li. Hence the larger the number of PO_4 groups around a given NbO_6 octahedron, the higher the value of the Nb^{5+}/Nb^{4+} redox couple. For both α-$NbPO_5$ and *β*-$NbPO_5$, four PO_4 tetrahedra share corners with one distorted NbO_6 octahedron, compared with six for the NASICON structure and only one for PNb_9O_{25}. Note also the important difference between the positions of the M^{5+}/M^{4+} redox couples in MPO_5 (M = V, Nb) structures: ∼4 V for V^{5+}/V^{4+},[7−9] ∼2 V for Nb^{5+}/Nb^{4+}. To our knowledge, *β*-Li_xNbPO_5 is the only one of these materials that do not show an extended biphasic behavior for the $0 \le x \le 1$ composition domain. Finally, one should notice that the ∼0.3 V difference between the Nb^{5+}/Nb^{4+} couples in α-$NbPO_5$ (∼1.65 V) and *β*-$NbPO_5$ (∼2.0 V) is of the same magnitude as that between the V^{5+}/V^{4+} couples in α-$VOPO_4$ (3.75 V)[29,31] and *β*-VPO_5 (4.00 V).[7]

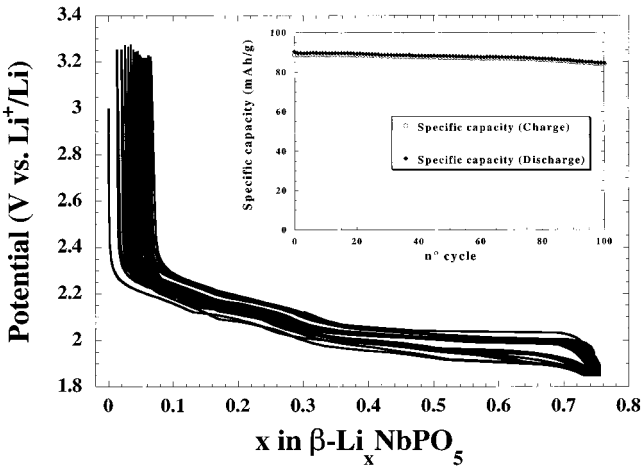

Figure 11. Charge−discharge profile under a galvanostatic mode at current density of C/5 (0.240 mA·h) in the 3.20−1.85 V range vs Li^+/Li for *β*-Li_xNbPO_5. The *inset plot* represents the evolution of the specific capacity over the first 100 cycles.

The electrochemical galvanostatic cycling data of α-$NbPO_5$ and *β*-$NbPO_5$ at a C/5 rate are plotted in Figures 10 and 11, respectively. The cutoff voltages had been chosen, as deduced from preliminary tests, in order to obtain the highest possible reversible capacity. At this rate, a strong polarization is noted for α-Li_xNbPO_5 with, as a consequence, a smearing out of the two-phase reaction at 1.7 V vs Li^+/Li. After an important irreversible capacity loss (∼50%) between the first discharge and the first charge, the cell shows a sustained 90 mA·h/g capacity over at least 50 cycles. The *β*-Li_xNbPO_5 system behaves much nicer. It shows a good reversibility and a remarkably low polarization for a relatively high rate (C/5) in the potential window 3.20−1.85 V, with an almost constant specific capacity of ∼90 mA·h/g. For extended discharges down to 1.7 V (i.e., $\Delta x \approx 0.9$) the specific capacity reaches 120 mA·h/g in the first cycles but rapidly decreases to reach 90 mA·h/g at the 45th cycle. This lower voltage cutoff-driven failure process

(28) Patoux, S.; Dolle, M.; Rousse, G.; Masquelier, C. *J. Electrochem. Soc.* **2002**, *149*, 391−400.
(29) Gaubicher, J. Thèse de l'Université Paris VI, 1998.
(30) Manthiram, A.; Goodenough, J. B. *J. Power Sources* **1989**, *26*, 403.
(31) Dupré, N.; Gaubicher, J.; Le Mercier, T.; Wallez, G.; Angenault, J.; Quarton, M. *Solid State Ionics* **2001**, *140*, 209−221.

is most likely linked to a progressive structural degradation upon cycling.

IV. Conclusion

The present work reports on the first comparative study of the electrochemical insertion of lithium into the two allotropic varieties of $NbPO_5$. Both compounds operate on the Nb^{5+}/Nb^{4+} redox couple situated at potentials between 2.2 and 1.5 V vs Li^+/Li. In house, in situ, X-ray diffraction coupled with GITT and PITT electrochemical cycling were particularly useful for differentiating the various stages of lithium intercalation. While the α-Li_xNbPO_5 variety shows a poor reversibility and a strong polarization along a mostly two-phase mechanism occurring in the range $\sim 0.4 < x < \sim 1.2$, whose the second phase seems very different from the pristine material, the β-Li_xNbPO_5 variety behaves in a much smoother and reversible way at an average potential ($\sim$2 V vs Li^+/Li), which is slightly higher than for the α-form ($\sim$1.6−1.7 V vs Li^+/Li). This enabled us to determine a voltage window into which the Li/β-Li_xNbPO_5 electrochemical system could be cycled with excellent capacity retention for over 100 cycles. Further work, already undertaken, will concentrate on the determination of the crystal structures of the new α′-Li_xNbPO_5 and β'-Li_xNbPO_5 intercalated phases electrochemically or chemically prepared.

CM010398D